

# Performance Evaluation of UWB Active-Passive Two-Way Ranging Distance Estimation Matrix Weighting Methods

Taavi Laadung<sup>1,2,\*</sup>, Sander Ulp<sup>2</sup>, Muhammad Mahtab Alam<sup>1</sup> and Yannick Le Moullec<sup>1</sup>

<sup>1</sup>Tallinn University of Technology, Ehitajate tee 5, Tallinn, 19086, Estonia

<sup>2</sup>Eliko Tehnoloogia Arenduskeskus OÜ, Aiandi 13/1, Tallinn, 12918, Estonia

## Abstract

This paper explores least squares (LS), median (MED), inverse distance weighting (IDW), distance weighted estimator (DWE) and three different weighted least squares (WLS) methods for Ultra-Wideband (UWB) active-passive two-way ranging (AP-TWR) measurement matrix estimation. The proposed methods were tested with practical experiments in line-of-sight (LOS) and two different non-line-of-sight (NLOS) conditions, and were benchmarked against an active-only single-sided two-way ranging (SS-TWR) method.

The results show that the proposed methods MED, IDW and DWE achieve comparable standard deviation values, while outperforming the root-mean-squared-error (RMSE) of SS-TWR ranging by up to 14.3% in LOS and 19.08% in NLOS conditions. The experiments validate that the MED, IDW and DWE methods for AP-TWR are NLOS-robust and achieve better RMSE performance than active-only SS-TWR ranging.

## Keywords

Active-Passive Two-Way Ranging, Ultra Wideband, Line-of-Sight, Non-Line-of-Sight

## 1. Introduction

During recent years, Ultra-Wideband (UWB) technology based positioning has been considered as an attractive and one of the most promising method to provide various location-based services. The increased interest for UWB can be explained by various traits that it offers: in addition to positioning, it can be also be used for data transfer, it provides high robustness to multipath, it does not strictly require line-of-sight (LOS) conditions, and it provides high accuracy in the order of centimeters [1].

Typically, UWB positioning is based on exploiting the propagation time of radio frequency signals due to the usage of temporally very short pulses. The main time-based methods are Time of Flight (ToF), which estimates the propagation time between two nodes, and time difference

---

*IPIN 2022 WiP Proceedings, September 5 - 7, 2022, Beijing, China*


\*Corresponding author.

✉ taavi.laadung@taltech.ee (T. Laadung); sander.ulp@eliko.ee (S. Ulp); muhammad.alam@taltech.ee (M. M. Alam); yannick.lemoullec@taltech.ee (Y. Le Moullec)

🆔 0000-0002-7909-5385 (T. Laadung); 0000-0002-3497-4204 (S. Ulp); 0000-0002-1055-7959 (M. M. Alam); 0000-0003-4667-621X (Y. Le Moullec)



© 2022 Copyright for this paper by its authors. Use permitted under Creative Commons License Attribution 4.0 International (CC BY 4.0).

 CEUR Workshop Proceedings (CEUR-WS.org)

of arrival (TDoA), which estimates the differences of arrival time of a signal between multiple nodes [2].

TDoA offers an air time advantage, where only a single packet per position estimate is needed, which decreases the overall energy consumption of the system and could theoretically support a high device density in the service area. The main disadvantage of TDoA is that the anchors of a system need to be synchronized very accurately, adding to the complexity of the system. Time of flight (ToF) estimates are typically achieved via two-way ranging (TWR) methods, which remove the need for tightly synchronized anchors at the expense of additional air time. This in turn increases the energy consumption and lowers the tag density in the service area [3].

In order to overcome the shortcomings of both methods, a compromise is found by using passive anchor nodes to assist in the positioning process. The estimates supplied by passive nodes allow to reduce the number of packets a system has to transmit in a TWR sequence, effectively allowing to reduce the energy consumption and increase the air time efficiency, while still benefiting from the relaxed anchor synchronization requirement.

For example, Hepp *et al.* in [4] provide an anchor-initiated active-passive ranging protocol, mounted on a quadcopter. Horváth *et al.* proposed another passive ranging method used in conjunction with double-sided (DS) TWR with an alternative calculation method for increased robustness [5]. These methods have been more focused on increasing the air time efficiency.

Although the seminal concept of tag-initiated Active-Passive Two-Way Ranging (AP-TWR) was published in [6], the concept of generalized tag-initiated AP-TWR was introduced in [7]. This method was further expanded in [8] to include an additional passive ranging method and assess the performance of AP-TWR in conjunction with different active ranging methods.

The main idea of AP-TWR is to employ *a priori* information about anchor locations to calculate extra passive range estimates in addition to standard TWR estimates, without any additional impact on the air time. When maximum air time efficiency is not critical, the system can be scaled such that multiple active anchors are used, so the ranging performance can be increased. The achieved range estimates can then be arranged in a measurement matrix, which holds all the ranging data for a single ranging sequence. The previous papers have only utilized averaging of the measurement matrix rows to provide final range estimates, without looking into other methods. Additionally, the experiments were exclusively in line-of-sight (LOS) propagation conditions [7, 8].

In this paper we investigate methods to further improve AP-TWR range estimation via the manipulation of the resulting measurement matrix. These methods are then compared in various locations, in LOS and two separate non-line-of-sight (NLOS) propagation conditions. The rest of this paper is structured as follows: in Section 2 we give the theoretical background for AP-TWR, Section 3 lists the estimation methods to process the measurement matrix, Section 4 provides information on the experimental test setup, Section 5 presents the experimental results and the analysis; finally, the conclusions are drawn.

## 2. AP-TWR

AP-TWR defines two types of anchors, active-passive and passive-only, the former taking part of the ranging via standard TWR methods and listening to other transmissions while

not transmitting. The second type of anchors only listen to ongoing transmissions in the air, providing range estimates without actively partaking in them.

The work in [8] defined separate AP1-TWR and AP2-TWR methods, where the results showed that AP2-TWR is the better performing method. Therefore, in the scope of this paper we will be focusing on this method, while calling it just AP-TWR in order to avoid confusion.

The UWB ranging protocol is pictured in Fig. 1, where tag T initiates a ranging sequence by starting its internal timer and transmitting an UWB frame to active anchor  $A_i$ , which starts its timer and responds after its processing time  $t_{A_i,T}$ . Upon receiving  $A_i$ 's reply, T sends out a final UWB frame after its processing time  $t_{T,A_i}$ . Passive anchor  $A_j$  listens in on all the transmissions during the ranging sequence and records the corresponding times.

All the relevant time intervals for AP-TWR are described in more detail after the introduction of (1). As per Fig. 1 and [8], the AP-TWR employing Single-Sided Two-Way Ranging (SS-TWR) active method is described as

$$t_{T \leftrightarrow A_j | A_i} = \begin{cases} \frac{t_{T,A_i} - t_{A_i,T}}{2}, & \text{for } i = j \\ \frac{t_{A_i,T} + t_{T,A_i}}{2} + t_{A_i \leftrightarrow A_j} - t_{A_j,A_i}, & \text{for } i \neq j, \end{cases} \quad (1)$$

where  $t_{T \leftrightarrow A_j | A_i}$  is the calculated time of flight (ToF) between the tag T and the  $j$ -th passive anchor  $A_j$ , while the  $i$ -th active anchor  $A_i$  is partaking in the ranging sequence. This distinction is made because a single passive anchor can produce an estimate of the ToF between T and  $A_j$  following each  $A_i$ 's response. In the special case where  $i = j$ , only the active range estimate can be calculated; in this case it is calculated using SS-TWR. This is done by time intervals  $t_{A_i,T}$  - the time interval measured by  $A_i$  corresponding to reception of T, and  $t_{T,A_i}$  - time interval measured by T corresponding to the reception of  $A_i$ . In other cases, the passive estimate is calculated using the above mentioned  $t_{A_i,T}$ ,  $t_{T,A_i}$ , the known ToF between  $A_i$  and  $A_j$  -  $t_{A_i \leftrightarrow A_j}$ , and  $t_{A_j,A_i}$  - the time interval measured by  $A_j$  corresponding to the reception of  $A_i$ .

Calculating all possible  $t_{T \leftrightarrow A_j | A_i}$  values via (1) results in the following  $n$ -by- $m$  ToF measurement matrix  $\mathbf{T}$ :

$$\mathbf{T} = \begin{bmatrix} t_{T \leftrightarrow A_1 | A_1} & \cdots & t_{T \leftrightarrow A_1 | A_m} \\ \vdots & \ddots & \vdots \\ t_{T \leftrightarrow A_n | A_1} & \cdots & t_{T \leftrightarrow A_n | A_m} \end{bmatrix}, \quad (2)$$

where  $\{i \in \mathbb{Z} : 1 \leq i \leq m\}$ ,  $\{j \in \mathbb{Z} : 1 \leq j \leq n\}$  and the total number of anchors  $n$  consists of the number of active-passive anchors  $m$  and passive-only anchors  $k$ , such that  $n = m + k$ .

It can be observed that the ToF estimates achieved via active TWR methods are located on the main diagonal of  $\mathbf{T}$ , and the passive estimates of AP-TWR are situated off the main diagonal, so rows  $\{j \in \mathbb{Z} : m < j \leq n\}$  contain only passive ToF estimates.

The active SS-TWR method, as a result of its shorter measurement period, provides a lower relative motion induced error than the effectively longer Asymmetric Double-Sided Two-Way Ranging (ADS-TWR). The larger error is on account of including the final frame of the tag in the calculation of the range estimate [9].

It can be observed from Fig. 1 that the duration of the frame exchange regarding the calculation of the passive range estimates is in the same range as SS-TWR, since the time intervals incorporating the third UWB frame of the tag are not used in (1). Therefore we can assume that the relative motion error for AP-TWR passive range estimates is lower than ADS-TWR, for example.

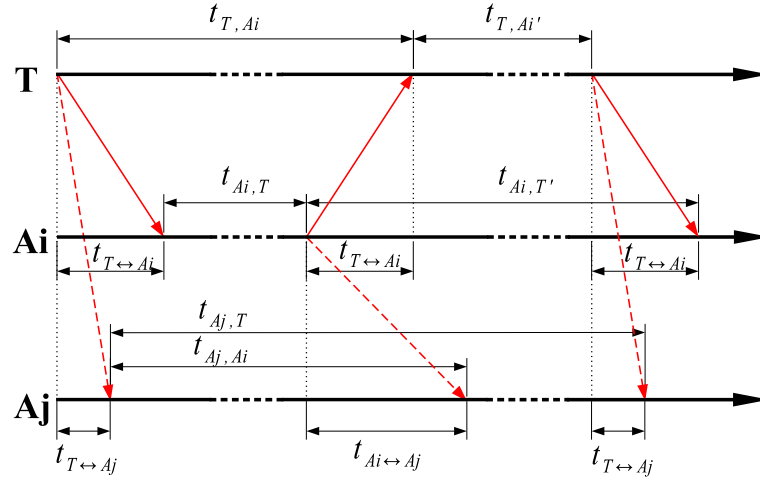


**Figure 1:** AP-TWR: Message exchange of tag T and active anchor Ai, while passive anchor Aj listens to the transmissions.

Moreover, assuming that the total length of the ranging protocol is in the order of milliseconds, we can infer that the error originating from the tag's relative movement to the anchors can altogether be omitted [10, 11].

AP-TWR cases  $m > 1$  produce a ToF estimate matrix (2) consisting of more than one column and row, where the elements of each row are individual estimates of the true ToF between T and Aj,  $t_{T \leftrightarrow Aj}$ . Considering all the above, we can assume that elements of each row are independent estimates of  $t_{T \leftrightarrow Aj}$ , the values of which can be considered as constants for the duration of a single ranging sequence.

The number of rows show the number of unique distance measurements between the tag and anchors, and the values in each row are separate estimates of a single anchor-to-tag distance value. That is, the number of columns represents the number of measurements that can be processed to provide a final range estimate for that specific anchor. The row values need to be processed in order to provide a more accurate, precise and robust final distance estimate.

The following section focuses on the methods of estimating the values of  $t_{T \leftrightarrow Aj}$  from the measurement matrix presented by (2).

### 3. Estimation methods

This section describes the methods of processing the raw measurement matrix values to achieve the final distance values as inputs for a positioning system. Many of the described methods

employ estimation of  $t_{T \leftrightarrow A_j}$  via calculating a weighted arithmetic mean, differing by only how the weights are generated.

The weighted mean (WM) of the  $j$ -th row of the measurement matrix can be expressed as:

$$WM(\overline{t_{T \leftrightarrow A_j | A_1 : m}}) = \frac{\sum_{i=1}^m (w_{j,i} \cdot t_{T \leftrightarrow A_j | A_i})}{\sum_{i=1}^m w_{j,i}}, \quad (3)$$

where  $w_{j,i}$  are the non-negative weights corresponding to each of the measurement matrix element  $t_{T \leftrightarrow A_j | A_i}$ . The special case where all the weights are equal, the solution simplifies to a standard arithmetic mean:

$$AM(\overline{t_{T \leftrightarrow A_j | A_1 : m}}) = \frac{\sum_{i=1}^m t_{T \leftrightarrow A_j | A_i}}{m}, \quad (4)$$

which will be discussed in the following Section.

### 3.1. Least Squares

In order to better describe the concept, we deconstruct the measurement matrix (2) to a set of  $n$  row vectors:

$$\begin{aligned} \mathbf{t}_{T \leftrightarrow A_1} &= [t_{T \leftrightarrow A_1 | A_1} \quad \cdots \quad t_{T \leftrightarrow A_1 | A_m}] \\ &\quad \vdots \\ \mathbf{t}_{T \leftrightarrow A_n} &= [t_{T \leftrightarrow A_n | A_1} \quad \cdots \quad t_{T \leftrightarrow A_n | A_m}] \end{aligned} \quad (5)$$

The problem of estimating the value of a constant using Least Squares (LS) is reduced to finding the mean value of the individual elements of the input vector [12]. The method is desirable because no additional information of the ToF estimates is needed and thus calculating weights is not needed.

As stated above, the LS solution for estimating a constant simplifies to calculating the arithmetic mean by applying (4) to (5):

$$\hat{T}_{LS} = \begin{bmatrix} \overline{t_{T \leftrightarrow A_1 | A_1 : m}} \\ \vdots \\ \overline{t_{T \leftrightarrow A_n | A_1 : m}} \end{bmatrix}, \quad (6)$$

where  $\hat{T}_{LS}$  is a vector containing  $n$  final LS estimates of the ToF between the tag and the anchors.

### 3.2. Median

Like in the previous section, we adopt the vector notation of (5) to provide the solution of the next method.

Then the vector of final ToF estimates can be found as the median values of each vector of (5) as follows:

$$\hat{T}_{MED} = \begin{bmatrix} \tilde{t}_{T \leftrightarrow A1|A1:m} \\ \vdots \\ \tilde{t}_{T \leftrightarrow An|A1:m} \end{bmatrix}, \quad (7)$$

where the tilde accent notes the mathematical operation of median, which does not require extra information on measurements, while being a more robust estimator in presence of outliers than LS.

### 3.3. Inverse Distance Weighting

The Inverse Distance Weighting (IDW) method was introduced by Shepard in [13], which was devised as an interpolation function to produce a continuous surface from discrete data points.

Following the idea of Shepard, we take the liberty to rewrite the concept of IDW into the context of the current paper:

$$t_{T \leftrightarrow Aj} = \begin{cases} \frac{\sum_{i=1}^m (t_{T \leftrightarrow Aj|Ai} \cdot d_{j,i}^{-1})}{\sum_{i=1}^m d_{j,i}^{-1}}, & \text{if } d_{j,i} \neq 0 \text{ for all } i, \\ \overline{t_{T \leftrightarrow Aj|A1:m}}, & \text{if } d_{j,i} = 0 \text{ for some } i, \end{cases} \quad (8)$$

where

$$d_{j,i} = |t_{T \leftrightarrow Aj|Ai} - \overline{t_{T \leftrightarrow Aj|A1:m}}|. \quad (9)$$

Equation (9) is the first-order distance function of  $t_{T \leftrightarrow Aj|Ai}$ . Since we are working in one dimension, the value of the distance function  $d_{j,i}$  is calculated as the absolute value of the difference of  $t_{T \leftrightarrow Aj|Ai}$  and the arithmetic mean of row  $j$ .

The value of  $d_{j,i}$  is in turn used in the calculation of the first-order IDW estimate by (8), where the order is specified by the magnitude of the negative exponent of  $d_{j,i}$ . Larger exponent values effectively give larger weight to ToF estimates which are closer to the arithmetic mean.

### 3.4. Distance Weighted Estimator

Dodonov and Dodonova introduced the Distance Weighted Estimator (DWE) in [14], which provides a robust estimate of central tendency without the need of separately calculating a mean value.

Adopting our notation to (9) of [14], we get the expression to calculate the DWE weights as follows:

$$w_{j,i} = \frac{m-1}{\sum_{l=1}^m |t_{T \leftrightarrow Aj|Ai} - t_{T \leftrightarrow Aj|Al}|} \quad (10)$$

where each of the weights are calculated as the inverse mean distance of  $t_{T \leftrightarrow A_j | A_i}$  and other elements of row  $j$ . These weights are in turn used in (3), to provide the set of final ToF estimates  $t_{T \leftrightarrow A_j}$ .

### 3.5. Weighted Least Squares 1

The solution to Weighted Least Squares (WLS) estimation reduces to weighting the measured values with their corresponding noise variance, keeping in mind that the noise for each measurement is considered zero-mean and independent [12].

Firstly, we consider the theoretical noise variance values as the basis for the weights to calculate an estimate for the WLS1 method.

Considering the results of [6, 8], we can assume that active ranging (SS-TWR and AltDS-TWR, respectively) performs at about 3.2 cm root-mean-square error (RMSE) and passive ranging of AP-TWR in the range of 5.2 to 5.5 cm RMSE.

The RMSE values are presented in centimeters to reflect the final product of ranging, as opposed to providing the RMSE in picoseconds for the ToF measurements. Both representations can be used interchangeably, since the ToF time  $t_{ToF}$  and the distance value  $d$  are related to each other via the propagation speed  $c$  (in this case, the speed of light) through the expression  $d = c \cdot t_{ToF}$ .

As the WLS solution employs weighting based on the noise variance, the WLS1 weights for the measurement matrix can be written as

$$w_{j,i} = \begin{cases} \frac{1}{\sigma_a^2}, & \text{for } i = j, \\ \frac{1}{\sigma_p^2}, & \text{for } i \neq j, \end{cases} \quad (11)$$

where  $\sigma_a^2$  is the variance of the active measurements, and  $\sigma_p^2$  is the variance of the AP-TWR passive measurements. The calculated weights  $w_{j,i}$  are in turn used in (3) for the calculation of the final estimate.

The calculation of RMSE and standard deviation is somewhat similar, where the former is calculated using the known true value and the latter employing the sample mean value [8]. Therefore when the true value is equal to the sample mean, the RMSE and standard deviation values are also equal. Assuming the same data, but where the true value is not equal to the sample mean, the RMSE value is higher than the standard deviation of the data set.

Therefore in the scope of this paper we assume the value of standard deviation for the passive range estimates at  $\sigma_p = 5.5$  cm, and for active estimates  $\sigma_a = 3.2$  cm, inferred from the RMSE results of previous papers.

### 3.6. Weighted Least Squares 2

Following the approach of weights calculated using the theoretical variances, we propose the second method of weighted least squares (WLS2).

Firstly, we find each elements' distance from their corresponding row mean of the ToF measurement matrix  $T$  by adopting (9). By doing so, we formulate a mean-shifted measurement matrix  $T_S$ :

$$T_S = \begin{bmatrix} d_{1,1} & \dots & d_{1,m} \\ \vdots & \ddots & \vdots \\ d_{n,1} & \dots & d_{n,m} \end{bmatrix}. \quad (12)$$

Since the newly formed  $T_S$  is centered around its mean values, we can calculate column-wise variances:

$$\sigma_i^2 = \frac{\sum_{j=1}^n (d_{j,i} - \overline{d_{1:n,i}})^2}{n}, \quad (13)$$

where  $\overline{d_{1:n,i}}$  is the mean value of column  $i$  of (12) and  $\sigma_i^2$  are the calculated column-wise variances. Then the according weights can be calculated as

$$w_{j,i} = \frac{1}{\sigma_i^2}, \text{ for all } j. \quad (14)$$

The weights calculated by this method are the same for each row of the measurement matrix, changing only with each successive ranging sequence. Similarly to the previous section, the resulting weights are then used in (3) for the final ranging estimates.

### 3.7. Weighted Least Squares 3

In this section, we propose a third method for Weighted Least Squares (WLS3), for which the noise variance-based weights are also calculated for each row separately.

In order to calculate the final weights, the measurement matrix needs to be centered via (12) and the column-wise variances calculated, similarly to the previous section. Then the row-wise variances of  $T_S$  need to be calculated as well:

$$\sigma_j^2 = \frac{\sum_{i=1}^m (d_{j,i} - \overline{d_{j,1:m}})^2}{m}, \quad (15)$$

where  $\overline{d_{j,1:m}}$  is the mean value of row  $j$ , and  $\sigma_j^2$  is the row-wise variance of the measurement matrix. Following the calculation of  $\sigma_i^2$  and  $\sigma_j^2$ , we then combine them into  $\sigma_{j,i}^2$  by the following expression:

$$\sigma_{j,i}^2 = \frac{\sigma_j^2 + \sigma_i^2}{2}. \quad (16)$$

Based on (16), we can then calculate the weights by

$$w_{j,i} = \frac{1}{\sigma_{j,i}^2}, \quad (17)$$

which are in turn used as weights in (3) for the final AP-TWR ranging estimates.



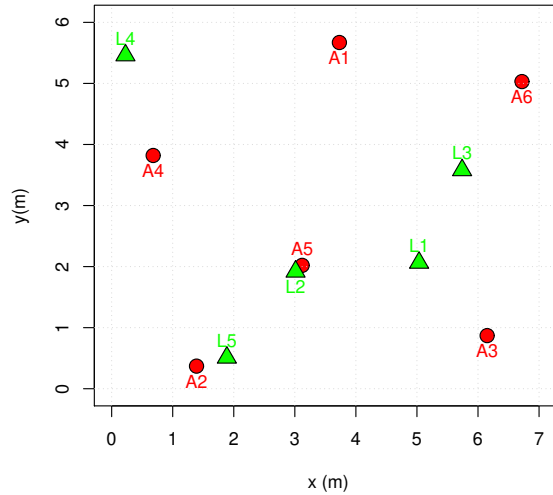


**Figure 2:** Representation of the test room setup in XY-plane. Anchors are marked with red circles and the test locations of the tag with green triangles.

## 4. Test Setup

In order to assess the performance of each of the previously specified methods, practical experiments were conducted. In this section we describe the preliminaries for the experiments.

The tests were ran in a 7.2 m by 6 m university laboratory room with concrete-walls, furnished with desks and computers. The UWB system used for experiments was the Eliko UWB RTLS [15] consisting of 6 active-passive anchors and a single tag. The active and passive range estimates were gathered via a laptop connected to the ranging engine of the Eliko UWB RTLS.

The active range estimates were attained using SS-TWR, and the passive estimates via the AP-TWR passive method described in Section 2. The gathered estimates were post-processed using a custom script written in R, implementing all the methods described in Section 3. Additionally, the script also calculates various statistical parameters, including RMSE and standard deviation, which are the basis for the results presented in Section 5. Apart from the proposed estimation methods, no additional filtering or trimming was applied to the measurement matrix.

The true coordinates of the anchors and of the tag at various positions were measured with a Leica Disto S910 laser distance meter [16]. In addition, the anchor-tag true distances were also verified with the Leica Disto S910, in order to calculate some of the needed performance parameters.

The data was gathered with a tag installed on a tripod at 5 arbitrarily chosen points in the room, which are marked on Fig. 2 alongside the locations of the anchors; the anchors are

**Table 1**

Test setup: anchors ( $A_x$ ) subjected to NLOS in the 5 test locations (Loc  $x$ ).

Loc 1	Loc 2	Loc 3	Loc 4	Loc 5
A1, A2, A4, A5	A2, A4	A1, A2, A4, A5	ALL	A3, A6

marked with red circles and the locations of the tag with green triangles.

In each location 3 separate tests were conducted: one line-of-sight (LOS) test and two separate non-line-of-sight (NLOS) tests. The NLOS tests were conducted by disrupting the LOS between anchors and a tag by either a 40 cm by 20 cm, 0.8 mm thick sheet of metal (NLOS1) or a human body chest area (NLOS2), placed at a distance of about 5 cm from the tag. Note that for both NLOS tests, the propagation paths to the same exact anchors were disrupted to have a fair comparison of the different NLOS conditions. Table 1 gives the details of NLOS tests, i.e. which anchors have NLOS propagation conditions at each of the test locations.

During each separate test, data from a minimum of 1200 separate ranging sequences were collected. Considering that the setup consisted of AP-TWR  $m = 6, k = 0$ , this amounts to at a minimum of 43200 raw range values across all the captured measurement matrices.

## 5. Experimental Results

The results of the experiments are given in Fig. 3, where the RMSE and standard deviation (SD) values for each of the test locations is given, depending on the propagation conditions. Fig. 3 a, b and c give the RMSE values for LOS, NLOS1 and NLOS2, respectively. Fig. 3 d, e, f give the respective SD values for the same propagation conditions. Additionally, a zoomed-in region of each of the sub-figures is given for location 4 since the traces can be placed quite densely.

Alongside the seven proposed methods (LS, Med, IDW, DWE, WLS1, WLS2, WLS3), the performance of active-only (SS-TWR) and AP-TWR passive-only ranging estimates from the same exact measurements is also given. They are separately pictured in order to give a baseline comparison of the performance of the proposed methods.

It can be observed from Fig. 3 a - c that the RMSE of passive measurements is almost always lower than the active-only method, with the exception of locations 1 and 2 in Fig. 3 a. On the other hand, the results for SD show the opposite: active-only estimates outperform the passive-only methods in every single test and location by a very slight margin. This is also in line with the results attained in previous publications regarding AP-TWR [6, 7, 8].

Although in regards of SD, the proposed methods' performance always places between the active and passive-only methods, the RMSE values show that many of the proposed methods provide better results than even the baseline better-performing passive-only estimates.

The average SD across all locations, depending on the method used, is shown as the bars on Fig. 4. From these results we can again see that the active estimates provide the lowest SD, while the passive estimates perform the least. The results from all three propagation condition tests show that utilizing the MED, IDW or DWE methods provide comparable performance to the most precise active-only estimates.

Across all locations the average RMSE values of LOS, NLOS1 and NLOS2 conditions depending on the method are given in Fig. 4, pictured by the lines+markers. The following analysis focuses on the RMSE improvements compared to a active-only SS-TWR method (Active method RMSE of Fig. 4), which achieved an RMSE of 24.209 cm in LOS, 36.006 cm in NLOS1 and 37.123 cm in NLOS2.

The WLS3 method provides the lowest RMSE of all the methods in LOS conditions at 20.742 cm (decrease of 14.3%), followed closely by IDW (20.785 cm, decrease of 14.14%) and DWE

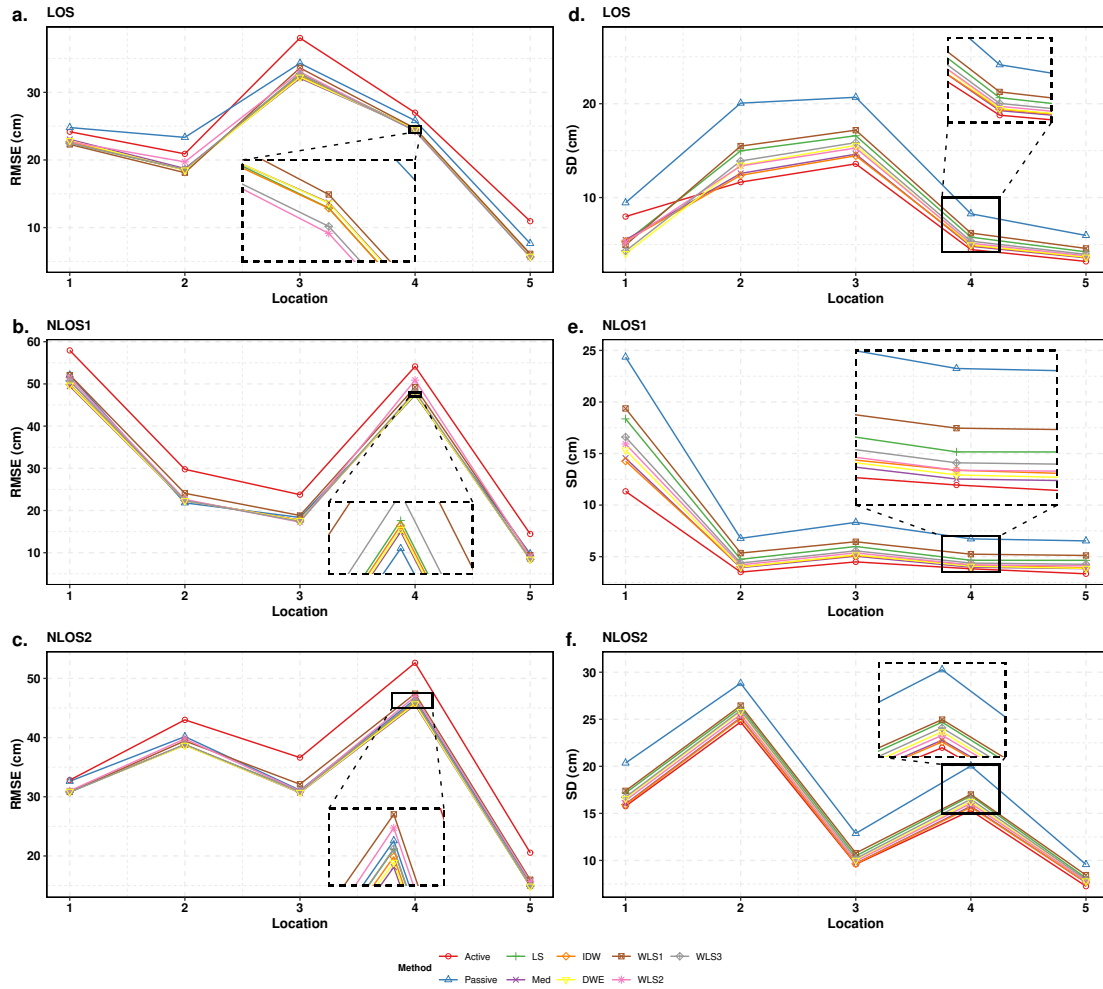


**Figure 3:** Results of experiments at each individual location. Parts a, b, c present the RMSE of the proposed methods in LOS, NLOS1 and NLOS2 propagation conditions; parts d, e, f present the respective standard deviation (SD) values. Lower is better for all of the figures, note the different scales on each figure.

(20.795 cm, decrease of 14.10%), up to the least performing method of WLS2 (21.064 cm, decrease of 13.00%). The results show that in LOS conditions all of the proposed methods perform similarly, with a difference of 0.322 cm between the best and worst performing method.

NLOS1 conditions showed the best performing method to be MED at 29.135 cm RMSE (decrease of 19.08%), followed by DWE at 29.169 cm (18.99% decrease) and IDW at 29.210 cm (18.87% decrease), with the lowest performing method WLS1 at 30.727 cm (14.66% decrease). It can be observed that in NLOS1 the absolute difference of the best and least performing methods, at 1.592 cm, is larger than in LOS.

NLOS2 conditions produced similar results where MED achieved the best results at 32.183 cm (13.31% decrease), followed by DWE at 32.190 cm (13.29%) and IDW at 32.251 cm (13.12%)

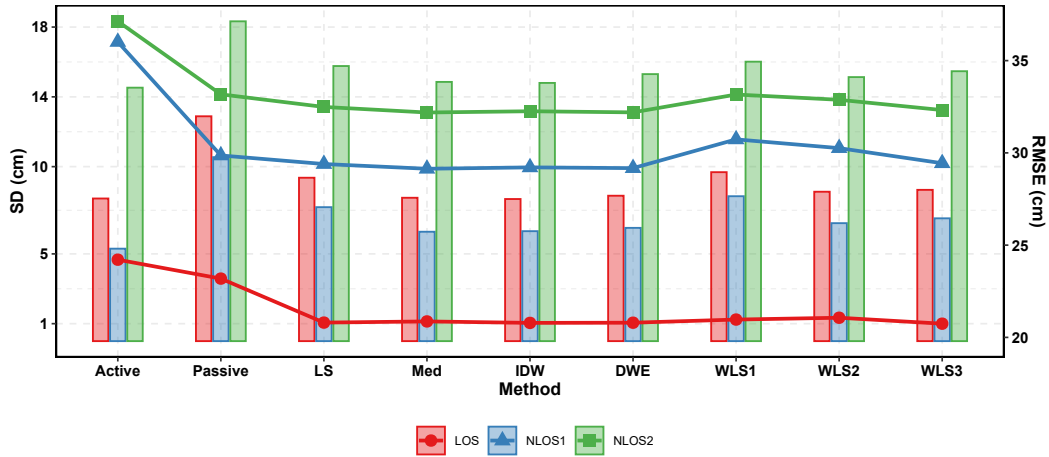


**Figure 4:** The average RMSE (lines+markers) and SD values (bars) for the proposed methods across all locations, depending on the tested propagation conditions. Lower is better.

with WLS1 landing at the last place with 33.157 cm RMSE (decrease of 10.68%). Similar to the previous result, the absolute difference of the methods is lower than NLOS1 but is still about 3 times as large as in LOS with 0.974 cm.

In terms of RMSE, the LS, MED, IDW and DWE methods show millimeter level differences between each other in LOS and NLOS, providing essentially the same performance. Coupled with the fact that MED, IDW and DWE offer comparable SD performance to active estimates, it can be claimed that the MED, IDW and DWE methods are the best-suited measurement matrix estimation methods.

Compared to results shown in previous papers reporting on AP-TWR [6, 7, 8], the attained RMSE values were slightly higher than expected. This is partly due to the fact that earlier papers ran only LOS tests, so naturally the added NLOS would provide degraded performance due to the impairment of propagation conditions, but the reported LOS results showed slightly lower performance as well.

This could be explained by some systematic errors introduced in the system. These errors could be attributed to imperfect calibration of antenna delays, range bias (effect of signal strength to the reported ranging value) [17], multipath propagation [18] or even errors originating from the physical orientation of the devices in regards to each other [19].

## 6. Conclusion

The experiments validated that all of the methods decrease the ranging RMSE in LOS propagation conditions, while also showing that NLOS propagation conditions do not break down the methods but rather increase the performance in demanding propagation conditions.

Results also showed that the selection of the specific method is not so critical in LOS conditions, as all the methods perform equivalently. The two tested NLOS conditions showed that in both, absolute values and relative decrease of RMSE, are further increased by selecting the appropriate

method, meaning that the choice of methods becomes more crucial for real-life applications experiencing mixed LOS/NLOS conditions.

In LOS, all the methods perform almost identically - achieving up to 14.3% lower RMSE when using WLS3 method compared to SS-TWR. NLOS conditions showed that up to 19.08% decrease of RMSE can be achieved compared to SS-TWR by employing MED to the measurement matrix, whereas the LS, IDW and DWE methods' performance lies within a few millimeters of it.

Comparing with the standard deviation of the best-performing SS-TWR active ranging, it was observed that the MED, IDW and DWE achieve comparable results, implicating that the precision of these methods is approximately on the same level. Meaning that these methods offer no significant degradation of the precision when compared to the active-only ranging.

In conclusion, across the tested LOS, NLOS1 and NLOS2 propagation conditions the methods MED, IDW and DWE showed similar SD, while providing considerably higher RMSE performance compared to SS-TWR. Taking into account these results it can be claimed that either one of the MED, IDW or DWE methods are sufficient for the AP-TWR measurement matrix estimation, while showing that these methods are also robust in NLOS conditions.

For future work, new experiments could be conducted in larger and more complex environments with harsher multipath effects present. Moreover, additional locations and tag orientations should be investigated to average out the device orientation errors and tests with varying number of active-passive anchors ( $m$ ) should be conducted to see how it affects the performance of the proposed methods.

## Acknowledgments

This project has received funding from the European Union's Horizon 2020 Research and Innovation programme under grant agreement No 951867, 101058505 and 668995. This research has also been supported in part by the European Regional Development Fund, Study IT in Estonia Grant, and Estonian Research Council under Grant PUT-PRG424.

## References

- [1] A. Alarifi, A. Al-Salman, M. Alsaleh, A. Alnafessah, S. Al-Hadhrami, M. A. Al-Ammar, H. S. Al-Khalifa, Ultra wideband indoor positioning technologies: Analysis and recent advances, *Sensors (Switzerland)* 16 (2016) 1–36. doi:10.3390/s16050707.
- [2] H. Liu, H. Darabi, P. Banerjee, J. Liu, Survey of wireless indoor positioning techniques and systems, *IEEE Transactions on Systems, Man and Cybernetics Part C: Applications and Reviews* 37 (2007) 1067–1080. doi:10.1109/TSMCC.2007.905750.
- [3] M. Ridolfi, S. van de Velde, H. Steendam, E. De Poorter, Analysis of the scalability of UWB indoor localization solutions for high user densities, *Sensors (Switzerland)* 18 (2018) 1–19. doi:10.3390/s18061875.
- [4] B. Hepp, T. Nægeli, O. Hilliges, Omni-directional person tracking on a flying robot using occlusion-robust ultra-wideband signals, in: *IEEE International Conference on Intelligent Robots and Systems*, volume 2016-Novem, 2016, pp. 189–194. doi:10.1109/IRoS.2016.7759054.

- [5] K. A. Horvath, G. Ill, A. Milankovich, Passive extended double-sided two-way ranging with alternative calculation, in: 2017 IEEE 17th International Conference on Ubiquitous Wireless Broadband, ICUWB 2017 - Proceedings, 2017, pp. 1–5. doi:10.1109/ICUWB.2017.8250972.
- [6] S. Shah, T. Demeechai, Multiple simultaneous ranging in IR-UWB networks, *Sensors (Switzerland)* 19 (2019) 1–14. doi:10.3390/s19245415.
- [7] T. Laadung, S. Ulp, M. M. Alam, Y. Le Moullec, Active-Passive Two-Way Ranging Using UWB, in: 2020 14th International Conference on Signal Processing and Communication Systems (ICSPCS), IEEE, 2020, pp. 1–5. doi:10.1109/ICSPCS50536.2020.9309999.
- [8] T. Laadung, S. Ulp, M. M. Alam, Y. L. Moullec, Novel Active-Passive Two-Way Ranging Protocols for UWB Positioning Systems, *IEEE Sensors Journal* 22 (2022) 5223–5237. doi:10.1109/JSEN.2021.3125570.
- [9] C. Lin, X. Jin, S. Mo, C. Hou, W. Zhang, Z. Xu, Z. Jin, Performance analysis and validation of precision multisatellite RF measurement scheme for microsatellite formations, *Measurement Science and Technology* 33 (2022). doi:10.1088/1361-6501/ac37ea.
- [10] Y. Jiang, V. C. Leung, An asymmetric double sided two-way ranging for crystal offset, in: Conference Proceedings of the International Symposium on Signals, Systems and Electronics, Crdpj 320552, 2007, pp. 525–528. doi:10.1109/ISSSE.2007.4294528.
- [11] J. Cano, G. Pages, E. Chaumette, J. LeNy, Clock and Power-Induced Bias Correction for UWB Time-of-Flight Measurements, *IEEE Robotics and Automation Letters* 7 (2022) 2431–2438. doi:10.1109/LRA.2022.3143202.
- [12] D. Simon, *Optimal State Estimation: Kalman, H Infinity, and Nonlinear Approaches*, Wiley-Interscience, USA, 2006.
- [13] D. Shepard, A two- dimensional interpolation function for irregularly- spaced data, in: Proceedings of the 1968 23rd ACM national conference, 1968, pp. 517–524.
- [14] Y. S. Dodonov, Y. A. Dodonova, Robust measures of central tendency: Weighting as a possible alternative to trimming in response-time data analysis, *Psikhologicheskije Issledovaniya* 5 (2011) 1–11.
- [15] Eliko Tehnoloogia Arenduskeskus OÜ, Eliko UWB RTLS, 2022. URL: <https://eliko.ee/uwb-rtls-ultra-wideband-real-time-location-system/>, accessed May 5, 2022.
- [16] Leica Geosystems AG, Leica DISTO S910 User Manual, 2019. URL: <https://shop.leica-geosystems.com/sites/default/files/2019-04/leica-disto-s910-user-manual-805080-808183-806677-en.pdf>, accessed May 5, 2022.
- [17] Decawave/Qorvo, APS011 Application Note: Sources Of Error In DW1000 Based Two-Way Ranging (TWR) Schemes, 2018. URL: <https://www.qorvo.com/products/d/da008446>, accessed July 13, 2022.
- [18] A. D. Preter, G. Goysens, J. Anthonis, J. Swevers, G. Pipeleers, Range bias modeling and autocalibration of an UWB positioning system, in: 2019 International Conference on Indoor Positioning and Indoor Navigation, IPIN 2019, IEEE, 2019, pp. 1–8. doi:10.1109/IPIN.2019.8911815.
- [19] P. Krapež, M. Vidmar, M. Munih, Distance measurements in uwb-radio localization systems corrected with a feedforward neural network model, *Sensors* 21 (2021) 1–18. doi:10.3390/s21072294.